Equation of state for hard *n*-alkane models: Long chains

C. Vega and L. G. MacDowell
Departamento de Quimica Fisica, Facultad de Ciencias Quimicas, Universidad Complutense, 28040 Madrid, Spain

P. Padilla
Chemistry Laboratory III, HC Ørsted Institute, Universitetsparken 5, DK-2100 Copenhagen, Denmark

An equation of state (EOS) for hard *n*-alkane models is proposed. This equation requires a previous knowledge of the second virial coefficient of the hard *n*-alkane model. Since the numerical determination of the second virial coefficient of chain molecules is computationally expensive, a new method for estimating the second virial coefficient of hard polymer models is proposed. This method yields predictions for the second virial coefficients in very good agreement with those determined numerically. In order to test the proposed equation of state, molecular dynamics simulations for repulsive *n*-alkane chains were performed. Excellent agreement was found between theoretical and simulated pressures for *n*-alkanes with up to 100 monomer units. The effect of changes in the torsional potential, bond angle, and bond length, on the equation of state of hard *n*-alkane models is analyzed. The equation of state is also extended to mixtures of hard *n*-alkane models. The proposed methodology provides an accurate equation of state for realistic models of hard *n*-alkane molecules. An empirical formula describing the EOS of repulsive *n*-alkane chains is given. © *1995 American Institute of Physics.* [S0021-9606(96)51501-7]

I. INTRODUCTION

During the last years, a great amount of effort has been devoted to the study of molecules with internal flexibility. Computer simulation studies of flexible chain models either by Monte Carlo (MC) or by molecular dynamics (MD) have appeared,[1–8] and the vapor–liquid equilibrium of flexible models has been computed recently.[9,10] From a theoretical point of view, the interest has been focused on the determination of an equation of state (EOS) for hard flexible models. It is expected that the attractive forces will be incorporated in a perturbative way. Five different theoretical approaches have been developed: the polymer reference interaction site model integral equation[11] (PRISM); an extension of the Flory theory to hard flexible models, denoted as the generalized Flory dimer theory[12,13] (GFD); the density functional (DF) theory;[14,15] and Wertheim's theory of association, which has been extended to allow for the study of hard flexible molecules[16–18] and is commonly named as either the Wertheim theory (W) or the bonded hard sphere (BHS) theory. The fifth theoretical scheme combines ideas of the scaled particle theory and those of the Wertheim theory, and will be denoted as modified Wertheim (MW). The MW theory uses the EOS proposed by Wertheim, but with the nonsphericity parameter α replacing the number of spheres of the system.[19–23] The freely jointed hard sphere model[12] has been the subject to which most of the treatments have been applied. Although this is an interesting model, it is not a good representation of real chain molecules such as *n*-alkanes, where the bond angles are fixed and the monomer units overlap. Some attempts of extending these theories to hard *n*-alkane models have recently appeared.[22–26] At this moment it is not clear which of the different proposed treatments, namely, PRISM, GFD, DF, W, or MW theories, provides a better description of the behavior of hard chain molecules, so that they can be considered as complementary. For the particular case of hard *n*-alkane models, we have recently showed that the MW theory provides a very accurate description of the equation of state from *n*-butane up to *n*-octane.[22,23] Motivated by this success, the extension of the MW treatment to longer *n*-alkane models and to binary mixtures appears as the natural next step. That constitutes the main purpose of this work.

The importance of having a good equation of state for hard *n*-alkane models and their mixtures should not be overlooked. Perturbation theories and empirical equations of state usually divide the total pressure in a contribution arising from the repulsive forces, and another arising from the attractive ones. Therefore, it is quite important to have good equations of state for the repulsive part. The importance of *n*-alkanes in the petrochemical industry is large and therefore the attempt of describing hard *n*-alkane models seems worthwhile. In addition to that, some interesting issues such as the role played by bond length, bond angle, and torsional potential on the equation of state of the repulsive *n*-alkane model may be explored.

The scheme of this paper is as follows. In Sec. II the extension of the MW theory to long *n*-alkane molecules is presented. In Sec. III a new method for estimating the second virial coefficient of a hard conformer is proposed. Section IV describes the main features of the MD simulations performed to test the theoretical predictions. In Sec. V the results are shown and discussed. Finally, Sec. VI is devoted to the conclusions of this work.

II. THE MODIFIED WERTHEIM EQUATION OF STATE

According to Wertheim's first-order perturbation theory, the equation of state of m jointed hard spheres is given by[16,17]

$$Z = \frac{p}{\rho k T} = (m) \frac{1 + y + y^2 - y^3}{(1-y)^3}$$
$$- (m-1) \frac{1 + y - y^2/2}{(1-y)(1-y/2)}, \qquad (1)$$

where m is the number of spheres composing the polymer molecule. The packing fraction y is defined as

$$y = \rho V, \qquad (2)$$

where V is the molecular volume and ρ is the number density defined as $\rho = N/V'$. N is the number of chains and V' is the total volume of the system.

The second virial coefficient B as obtained from Eq. (1) is given by[19]

$$B/V = 1.5m + 2.5. \qquad (3)$$

Boublik[19] has shown that virial coefficients obtained from Eq. (1) are linear functions of m. According to Eq. (1), the EOS and virial coefficients of m jointed hard spheres do not depend on the bonding angle between the spheres and depend only on the number of spheres forming the molecule. This is obviously an approximation. For instance, for a rigid linear molecule (bonding angle equal to 180°), the fourth virial coefficient becomes negative[27] for large values of m, whereas Eq. (1) predicts positive values. Second, rigid linear molecules form liquid–crystal phases[28] for large m, whereas flexible models such as the freely jointed hard sphere do not form liquid–crystal phases[7] for m as large as 200.

A body is called convex if any line segment connecting two points on the surface of that body is completely contained within that body. For a convex body there is one and only one plane which is in contact with the surface of the convex body and whose normal is along the direction defined by the polar angles (Θ, Φ). This is called the supporting plane for the direction especified by (Θ, Φ). The perpendicular distance from the origin (located inside the body) to the supporting plane is denoted as the supporting function. The mean radius of curvature, R, is just the average of the supporting function over all possible directions defined by the polar angles (Θ, Φ). Further details concerning convex body geometry may be found elsewhere.[29–31] In scaled particle theories of hard convex molecules, it is common to define a nonsphericity parameter α as

$$\alpha = RS/3V, \qquad (4)$$

where S is just the area of the surface of the molecule. It can be proved rigorously that the second virial coefficient of a hard convex particle is given by[29–31]

$$B/V = 1 + 3\alpha. \qquad (5)$$

Therefore, for hard convex bodies Eq. (4) or (5) can be considered as the definition of α, since both yield identical results. For hard nonconvex particles the mean radius of curvature, R, is ill defined, and therefore Eq. (4) is not a suitable definition for α. The reason is that in a nonconvex body there are several planes tangent to the surface and whose normals are along the direction defined by the polar angles (Θ, Φ). This problem is usually overcome using any of the two following approaches:

Criterion 1: Equation (4) is kept as the definition of α, but R is taken to be the mean radius of curvature of a convex body of "similar" shape to that of the original nonconvex molecule.

Criterion 2: In this case, one takes notice of the fact that B is well defined for either convex or nonconvex molecules. Thus, one can use Eq. (5) as the definition of α, regardless of the shape of the molecule. This was first proposed by Rigby.[32]

For nonconvex bodies, these two choices yield slightly different values of α, but the differences are rather small provided that a reasonable choice for the mean radius of curvature is made. For instance, for hard diatomic molecules these two criteria yield values of α which differ about 3%.[29]

The connection between Wertheim's treatment of hard polymer models and scaled particle theory was made by Boublik,[19,20] and independently by Walsh and Gubbins.[21] These authors were able to show that for the freely jointed model, the second virial coefficient of Wertheim's EOS, given by Eq. (3), is identical to that given by Eq. (5) provided that α is defined through criterion 1 and R is taken as that of the spherocylinder enveloping the chain in its linear configuration. With this approximation it can be shown that, for the freely jointed hard sphere model, m and α are related by

$$m = 2\alpha - 1. \qquad (6)$$

By replacing Eq. (6) into Eq. (1) one obtains

$$Z = (2\alpha - 1) \frac{1 + y + y^2 - y^3}{(1-y)^3} - (2\alpha - 2) \frac{1 + y - y^2/2}{(1-y)(1-y/2)}. \qquad (7)$$

Equation (7) will be denoted as the modified Wertheim equation. With the choice made by Boublik and Walsh for α of a freely jointed hard sphere model, Eq. (7) reduces to Eq. (1). An important advantage of Eq. (7) over Eq. (1) appears when dealing with hard polymer models in which overlapping between bonded monomers is allowed. In this case, the nonsphericity parameter can be estimated and inserted into Eq. (7), whereas it is not so clear how to define the parameter m to be used in Eq. (1). Therefore, one of the main applications of Eq. (7) is the study of hard polymers where there is overlapping between bonded spheres. In fact, Eq. (7) has been tested with quite good results for a number of hard models,[20,21] and for realistic models of hard *n*-alkanes.[22,23]

In this work we are interested in obtaining an equation of state for a polymer model which is composed of monomeric units with fixed bond length, and with a Hamiltonian H described as

$$H = H_{\text{intra}} + H_{\text{inter}}, \qquad (8)$$

$$H_{intra} = \sum \frac{1}{2} k_\theta (\cos(\theta) - \cos(\theta_e))^2 + \sum_i u_{tor}(\phi_i)$$

$$+ \sum_{intra} u_{rep}(r_{ij}), \tag{9}$$

$$H_{inter} = \sum_{inter} u_{rep}(r_{ij}), \tag{10}$$

where k_θ is the force constant of the bending potential for the bond angle θ, θ_e is the equilibrium bond angle, $u_{tor}(\phi)$ is the torsional potential, which depends on the value of the torsional angle ϕ, and u_{rep} means a short-range repulsive site–site potential, for instance, a hard sphere site–site model, or the repulsive potential proposed by Weeks, Chandler, and Andersen[33] (WCA). Obviously this is a formidable problem which can only be tackled after some approximations. Our theoretical approach in search of an equation of state for the system described by Eqs. (8)–(10) can be stated as follows:

(i) We shall fix the bond angles to their equilibrium values. In Ref. 23 it was shown that bending vibrations do not affect much the equation of state of the n-alkane, provided that the bending constant k_θ is sufficiently large. Therefore, fixing bond angles to the equilibrium geometry appears as a reasonable approximation.

(ii) Following our treatment of Ref. 22, each molecule will be treated within the rotational isomeric state approximation[34] (RIS). For instance, for an n-alkane model three rotational states, trans (*t*), gauche$^+$ (g^+), and gauche$^-$ (g^-) are defined for each torsional degree of freedom. We assign a certain energy to the gauche state with respect to the trans state, and this energy is denoted as D, which is a function of the temperature, and a functional of the torsional potential used.[22] Within the RIS approximation, the system is regarded as a multicomponent mixture. For instance, *n*-butane is regarded as a mixture of trans, gauche$^+$ and gauche$^-$ conformers.

(iii) The next step is the estimation of the second virial coefficient of the system. The second virial coefficient of a multicomponent mixture is given by

$$B = \sum_{i,j} x_i x_j B_{ij}, \tag{11}$$

where x_i and x_j are the molar fractions of conformers i and j, respectively, and B_{ij} is the second virial coefficient between conformer i and conformer j. Unfortunately, Eq. (11) is still quite involved for practical calculations. The number of virial coefficients, B_{ij}, to be evaluated increases rapidly with the length of the chain. By approximating B_{ij} as

$$B_{ij} = \frac{(B_{ii} + B_{jj})}{2}. \tag{12}$$

Equation (11) can be rewritten as:

$$B = \sum_i x_i B_{ii}. \tag{13}$$

We shall define now the nonsphericity parameter of a given conformer i, α_i, by the criterion 2 so that

$$B_{ii}/V_i = 1 + 3\alpha_i, \tag{14}$$

where V_i stands for the volume of conformer i. By replacing Eq. (14) into Eq. (13),

$$B = \sum_i x_i (V_i + 3\alpha_i V_i). \tag{15}$$

In what follows we shall denote the average value of a given property A as $\bar{A}$, and will by obtained from the relation

$$\bar{A} = \sum x_i A_i \tag{16}$$

so that

$$B = \bar{V} + 3\overline{\alpha V}. \tag{17}$$

Since the different conformers of an n-alkane differ significantly in α_i but not in V_i, Eq. (17) can be approximated as

$$B = \bar{V} + 3\bar{\alpha}\bar{V} \tag{18}$$

or, finally,

$$B/\bar{V} = 1 + 3\bar{\alpha}. \tag{19}$$

Equation (19) allows an estimation of the second virial coefficient of a hard n-alkane model. The only requirement is the knowledge of the second virial coefficient B_{ii}, and volume V_i, of each conformer i of the flexible model. Since we are using criterion 2 for defining α_i we can also state that an estimation of the second virial coefficient of the hard flexible model can be achieved, if the nonsphericity parameter of the different conformers is known. We emphasize that Eq. (19) is not exact, but it should provide a reasonable estimate of the true second virial coefficient B which is given by Eq. (11).

(iv) The EOS of the system described by Eqs. (8)–(10) is obtained by replacing V by $\bar{V}$, and α by $\bar{\alpha}$ in Eq. (7). Therefore, the EOS proposed in this work is given by

$$Z = (2\bar{\alpha} - 1)\frac{1 + y + y^2 - y^3}{(1-y)^3} - (2\bar{\alpha} - 2)\frac{1 + y - y^2/2}{(1-y)(1-y/2)}, \tag{20}$$

$$\bar{\alpha} = \sum x_i \alpha_i, \tag{21}$$

$$y = \rho \sum x_i V_i = \rho \bar{V}. \tag{22}$$

It should be understood that the molar fraction of each conformer, x_i, is computed at zero density (ideal-gas population), and therefore it is a function of the temperature but not of the density. In previous work[23] it has been shown that changes of x_i with density at a given temperature are small, and therefore the use of the ideal-gas population for defining the average $\bar{\alpha}$ introduces little error in the computed equation of state. The second virial coefficient obtained from Eq. (20) is given by Eq. (19). Therefore, one expects good results for the equation of state at low densities when Eq. (20) is used.

The scheme represented by steps (i)–(iv) has been applied for hard *n*-alkanes up to *n*-octane.[22,23] In Ref. 22 the second virial coefficients of the different conformers of a hard *n*-alkane model were computed numerically, and the predictions from Eq. (20) were compared with simulation results for *n*-butane and *n*-pentane. The theory was further tested[23] by comparing simulation results of *n*-hexane, *n*-heptane, and *n*-octane with the theoretical results obtained from Eq. (20). The results were again quite good. It would be quite useful if the theory could be extended to longer *n*-alkanes.

There are two problems in extending the theory described by steps (i)–(iv) to longer *n*-alkanes models. The first problem arises from the fact that a complete enumeration of the conformers of an *n*-alkane becomes almost impossible for large *n* (the number of conformers of an *n*-alkane model grows as $3^{n-3}/2$). The second problem is that the exact evaluation of B_{ii} (and hence of α_i) for each conformer must be performed numerically, as shown in Ref. 22. The numerical evaluation of B_{ii} for a given conformer of, say, *n*-octane, takes several hours of CPU time in a common workstation. Therefore, the rigorous evaluation of $\bar{\alpha}$ cannot be achieved with the present computational resources. However, we shall show how the problem can be treated if Eqs. (21) and (22) are somewhat modified for long chains. An interesting observation is that in order to use Eq. (20), all what is needed is $\bar{\alpha}$ and $\bar{V}$ as defined by Eqs. (21) and (22). The evaluation of $\bar{\alpha}$ and $\bar{V}$ requires (within the RIS approximation) to sum in Eqs. (21) and (22) over all possible conformers of the system. However, a good estimation of the average can be obtained even if the summation in Eqs. (21) and (22) is restricted over some representative (i.e., large x_i) conformers of the system. Notice that the same idea is used in computer simulations, where reliable thermodynamic averages are obtained by sampling small regions of the phase space, instead of exploring exhaustively the phase space of the system. We can therefore perform a relatively short Monte Carlo simulation of an isolated chain, generating, say, 50 000 conformers, and take the true average of the volume and nonsphericity parameter as the average over the Monte Carlo run. We emphasize that our Monte Carlo refers to only one molecule, since we are evaluating ideal-gas averages. For obtaining $\bar{V}$, the volume of each individual conformer, V_i, is computed by using the efficient algorithm proposed by Dodd and Theodorou.[35] In order to compute $\bar{\alpha}$, the nonsphericity parameter of the individual conformers, α_i, must be determined. According to Eq. (14) that requires the value of the second virial coefficient for each individual conformer. It is not convenient to evaluate the exact second virial coefficients of each conformer generated in the MC run, since that would take a huge amount of computer time. From this discussion it is clear that a fast algorithm to estimate the second virial coefficient of a given conformer of a long chain is also required. Only in this way could the average value of $\bar{\alpha}$, be computed in a reasonable amount of time. Therefore our step (iv) of the theory is modified for long chains:

(iv) The EOS of the system is given by Eq. (20). To obtain $\bar{\alpha}$ and $\bar{V}$ a MC simulation of an isolated chain will be performed. For each conformer the values of V_i and B_{ii} (or α_i) are evaluated. The average values $\bar{V}$ and $\bar{\alpha}$ are obtained at the end of the MC run. In order to keep the computer time of the MC run within reasonable limits, the evaluation of α_i of each individual conformer must be obtained with little computational effort.

All that is now needed for a full development of the theory is a method for estimating the second virial coefficient B_{ii} (or α_i) of a given conformer of a long chain molecule. An empirical method for estimating α_i is presented in the next section.

III. ESTIMATING VIRIAL COEFFICIENTS OF HARD CHAIN CONFORMERS

In this section an empirical procedure to estimate the second virial coefficient of the different conformers of a flexible molecule will be proposed. In this work α_i of a given conformer or molecule will be defined through Eq. (14), and therefore the estimation of the second virial coefficient corresponds to the estimation of the nonsphericity parameter α_i.

In order to estimate α_i we shall use Eq. (4). The molecular volume V and surface S will be evaluated analytically by using the algorithm proposed by Dodd and Theodorou.[35] In general, the conformers appearing in a flexible hard chain are nonconvex bodies. Therefore, their mean radii of curvature are ill defined. This problem is usually overcome by taking the mean radius of curvature of a convex body with a similar shape to that of the molecule. Alejandre *et al.*[36] have proposed a numerical algorithm to evaluate the mean radius of curvature of the convex body enveloping the nonconvex molecule. This algorithm was used[37] to evaluate the nonsphericity of the different conformers of *n*-butane. The evaluation of R with the algorithm of Alejandre *et al.* is computationally faster than the evaluation of the second virial coefficient of the model. As it will be shown later, the algorithm of Alejandre *et al.* for determining R provides good estimates of the second virial coefficient of short hard *n*-alkane models, but it seems to deteriorate for longer ones. Therefore, an algorithm for determining R with accuracy for short and long hard *n*-alkane chains is needed. We shall describe an algorithm which satisfies this condition.

In this work, the mean radius of curvature, R, will be taken from a parallelepiped with sides a, b, and c. The parallelepiped is a convex body, so that its mean radius of curvature is well defined. The mean radius of curvature of a parallelepiped of sides a, b, and c is given by[38]

$$R = \frac{a+b+c}{4}. \tag{23}$$

The problem is how to obtain a, b, c. It would be desirable that the parallelepiped have a similar shape to that of the molecule. One possibility is to choose the parallelepiped so that its three principal moments of inertia match those of the conformer. We shall use this choice in the present work.

The three principal moments of inertia, I_1^p, I_2^p, and I_3^p, of a parallelepiped with sides a, b, c, total mass M, and uniform density through all the body are given by[39]

$$I_1^p = \frac{M}{12}(b^2 + c^2), \tag{24}$$

$$I_2^p = \frac{M}{12}(a^2 + c^2), \tag{25}$$

$$I_3^p = \frac{M}{12}(a^2 + b^2). \tag{26}$$

Now the three principal moments of inertia of the hard conformer, I_1^c, I_2^c, and I_3^c, should be calculated. This will be done by calculating the three eigenvalues of the inertia tensor. The hard conformer is made up of hard spheres. We shall assume that all the spheres have equal mass, and that the mass is homogeneously distributed within each sphere. The reason for this is that we are trying to reproduce the shape of the molecule and this goal is better achieved if the mass of each nuclei is spread through all the site. According to that, the element i,k of the inertia tensor $I_{i,k}$ is calculated as[39]

$$I_{i,k} = \sum_{l=1}^{n} \mu_l \left[\left(\frac{2}{5}\left(\frac{d_l}{2}\right)^2 + \sum_j (r_j^l)^2 \right) \delta_{i,k} - r_i^l r_k^l \right], \tag{27}$$

where μ_l and d_l are the mass and diameter of site l, respectively, $\delta_{i,k}$ stands for Kronecker's delta, r_i^l is the ith coordinate of site l referred to the center of masses of the molecule, and n is the number of monomer units. Although in this work we focus on chains made up of identical sites (so that $\mu_l = \mu$ and $d_l = d$ for all the monomer units), in the case of a polymer with different monomer units, the mass of each site should be proportional to the volume of the site. This is so, because the contribution of each site to the general shape of the molecule is proportional to its volume, but not to its mass, which is an irrelevant variable when describing the molecular shape (i.e., a heavy and very small atom makes a small contribution to the molecular shape). Once the principal moments of inertia of the conformer are known, these are equated to those of a parallelepiped of equal mass, thus obtaining the parameters a, b, and c required for the evaluation of R:

$$I_1^p = I_1^c, \tag{28}$$

$$I_2^p = I_2^c, \tag{29}$$

$$I_3^p = I_2^c. \tag{30}$$

In Eqs. (28)–(30) the total mass of the parallelepiped, M, was set equal to the mass of the *n*-alkane, given by $n\mu$. Once a, b, and c are obtained from Eqs. (28)–(30), then R is obtained from Eq. (23). Thus our procedure to estimate α_i can be summarized by saying that we use Eq. (4), taking S and V as the surface and volume of the conformer, and R as the radius of curvature of a parallelepiped with principal moments of inertia identical to those of the conformer. The estimate of α_i for a given conformer requires very little computational effort. In Table I estimates of α_i for some *n*-alkane

TABLE I. Nonsphericity parameters α_i of hard models of *n*-hexane, and *n*-heptane conformers as determined from Eq. (4), from Eq. (34), and from the method of Alejandre *et al.* (see Ref. 36). Exact values are taken from the second virial coefficients of Ref. 22.

	Exact	Eq. (4)	Eq. (34)	Alejandre
ttt	1.4253	1.4495	1.4174	1.4398
ttg	1.3795	1.4119	1.3799	1.3889
tgt	1.3807	1.4064	1.3743	1.3946
tgg	1.3215	1.3613	1.3292	1.3389
gtg	1.3282	1.3701	1.3380	1.3415
gtg'	1.3371	1.3695	1.3374	1.3541
ggg	1.2758	1.3192	1.2871	1.3031
tttt	1.5287	1.5506	1.5175	1.5459
tttg	1.4821	1.5130	1.4799	1.4959
ttgt	1.4813	1.5092	1.4761	1.4897
ttgg	1.4227	1.4622	1.4291	1.4358
tgtg	1.4310	1.4672	1.4341	1.4475
tgtg'	1.4412	1.4659	1.4328	1.4599
tggt	1.4165	1.4532	1.4201	1.4294
gttg	1.4360	1.4746	1.4415	1.4426
gttg'	1.4191	1.4646	1.4315	1.4246
tggg	1.3745	1.4146	1.3815	1.3993
gttg	1.3423	1.4088	1.3757	1.3727
gtg'g'	1.3839	1.4230	1.3899	1.4056
gggg	1.3307	1.3721	1.3390	1.3657

conformers obtained from Eq. (4) are compared with their exact values [obtained from Eq. (14) and the data of Ref. 22]. The model is that described in Ref. 22. It can be seen that Eq. (4) yields quite reasonable estimates of α_i. Moreover, when the nonsphericity parameter of the all trans conformer (*tt..t*) is subtracted from that of the other conformers of Table I, it can be seen that the differences obtained through our estimate agree quite well with the exact ones. This is important, since it indicates that the theory is especially good in describing differences in the nonsphericity parameter between the different conformers. That suggests that the estimate of α_i can be further improved. In fact, if the second virial coefficient of a given conformer (say, the all trans conformer) is known, the difference of nonsphericity between such a conformer and the all trans conformer can be estimated by using Eq. (4). Thus, a better prediction of α_i for the considered conformer is obtained. This improved prediction of α_i for a given conformer i can be written as

$$\alpha_i = \alpha_{tt..t} + \left(\frac{R_i S_i}{3 V_i} - \frac{R_{tt..t} S_{tt..t}}{3 V_{tt..t}} \right), \tag{31}$$

where the subindex $tt..t$ stands for the all trans conformer. For applying Eq. (31) the second virial coefficient of the all trans conformer (and hence $\alpha_{tt..t}$) must be known. In principle, B of the all trans conformer could be evaluated numerically. However, an even simpler procedure yields quite good results. The all trans conformer is an almost linear molecule. Therefore it is a good idea for this particular conformer to take R as that of a spherocylinder of length L and width d. For L we take the distance between the first and last monomeric units in the all trans configuration. The mean radius of curvature of a spherocylinder of length L and width d is given by[29]

TABLE II. Compressibility factor Z of repulsive *n*-alkane models. n is the number of carbon atoms . The reduced density is $\rho^* = N/V'\sigma^3$. Z_{Theory}, and Z_{MD} are theoretical [from Eq. (20)] and simulation results, respectively. The simulation results were obtained for the WCA model described in Sec. IV. MD results for $n=6, 7, 8$ were taken from Ref. 23 while those for $n=12, 16, 30$ were obtained in this work. For C_{50}, and C_{100} results were obtained for the *n*-alkane model of Ref. 5. Simulation results for C_{50}, and C_{100} were taken from Ref. 5. MD results for equimolar mixtures of WCA *n*-alkane models are also given. The 10+6 mixture denotes an equimolar binary mixture of C_{10}, and C_6.

n	ρ^*	Z_{MD}	Z_{Theory}
6	0.11815	3.1(1)	3.04
6	0.20085	7.25(8)	7.11
6	0.2954	20.7(1)	21.19
7	0.10042	3.15(6)	3.09
7	0.17722	8.07(8)	7.80
7	0.25401	21.45(9)	21.83
8	0.08861	3.26(6)	3.23
8	0.15359	8.1(1)	7.98
8	0.2245	23.0(2)	23.57
12	0.030796	1.99(7)	1.98
12	0.076991	5.45(6)	5.41
12	0.123185	14.85(13)	14.89
16	0.023445	2.17(10)	2.18
16	0.058613	6.42(8)	6.38
16	0.093781	17.98(18)	18.21
30	0.012773	2.80(8)	2.80
30	0.031933	9.80(9)	9.56
30	0.051093	28.88(24)	29.05
50	0.04699	118.2	127.96
100	0.02353	217.64	213.59
10+6	0.08861	3.27(7)	3.23
10+6	0.15359	8.10(6)	7.98
10+6	0.22450	23.00(7)	23.59
12+4	0.08861	3.27(6)	3.24
12+4	0.15359	8.09(6)	8.02
12+4	0.22450	23.00(7)	23.72

$$R = \frac{L}{4} + \frac{d}{2}. \tag{32}$$

For the all trans conformer, $\alpha_{tt..t}$ can be estimated with very good results as

$$\alpha_{tt..t} = \frac{(L/4 + d/2)S_{tt..t}}{3V_{tt..t}}. \tag{33}$$

By replacing Eq. (33) into Eq. (31) one obtains

$$\alpha_i = \frac{R_i S_i}{3V_i} + \frac{(L/4 + d/2 - R_{tt..t})S_{tt..t}}{3V_{tt..t}}. \tag{34}$$

Equation (34) is the working expression for the estimate of α_i proposed in this work. The subindex i stands for the properties of the conformer i. In Table I the value of α_i, as estimated from Eq. (34), is compared with the exact value of α_i from Ref. 22. It can be seen that Eq. (34) yields quite good predictions of the second virial coefficient of the different conformers of the hard *n*-alkane model. This is important since Eq. (34) reduces the computational effort of determining α_i by several orders of magnitude with respect to a rigorous evaluation of the second virial coefficient of the conformer. We also include in Table I the estimate of α_i from

the procedure proposed by Alejandre *et al.*[36] These authors used Eq. (4) for estimating α_i but with a different choice for R. It is seen that the estimate of α_i from the method of Alejandre *et al.*[36] is in good agreement with the exact values of α_i. Therefore Eq. (34) and the method of Alejandre *et al.* yield similar predictions of α_i for short hard *n*-alkane conformers. However, for long chains, estimates of the nonsphericities obtained from Eq. (34) and from the methodology of Alejandre *et al.* differ significantly. For instance, for the model of C_{30} described in the next section, the values of $\bar\alpha$ [see Eq. (21)] obtained from Eq. (34), and from the method of Alejandre *et al.* are 3.6838 and 3.2967, respectively. In order to elucidate which one of these two methods gives the best prediction for $\bar\alpha$, low-density results for the equation of state, obtained from Eq. (20), using the two values of $\bar\alpha$ mentioned above, were compared with MD simulation results. It was found that, whereas the value 3.6838 yields quite good agreement with the MD results, the value 3.2967 yields too low pressures. Although this test is not conclusive it suggests that Eq. (34) yields better predictions of the second virial coefficients than the method of Alejandre *et al.* Therefore, in what follows Eq. (34) will be used as the estimate of α_i for a given conformer. The contribution of the correction [second term on the right-hand side of Eq. (34)] is important for hard *n*-alkanes models with less than 16 carbon atoms, and becomes very small for longer chains. Therefore, for chains longer than 30 carbon atoms the second term on the right-hand side of Eq. (34) can be neglected.

Our algorithm for the determination of the EOS of the molecule can be summarized as:

(1) Use of Wertheim's EOS with m replaced by $2\bar\alpha - 1$ and V by $\bar V$, as shown in Eq. (20).

(2) The average value of the nonsphericity, $\bar\alpha$, and volume $\bar V$ are obtained from a Monte Carlo run of an isolated chain with fixed bond lengths and angles, and with torsional degrees of freedom treated within the RIS approximation. If the model presents intramolecular interactions they will be included in the MC run.

(3) The value of α_i for each conformer appearing in the Monte Carlo run is estimated from Eq. (34).

In order to check the proposed algorithm some MD simulations have been performed for *n*-alkane chains. In the next section some details concerning these simulations are given.

IV. SIMULATION METHODOLOGY

The theory described in Secs. II and III can be applied to hard polymer models. Hard models are not very convenient for MD simulations since the potential is discontinuous. Because of that, MD simulations were performed for a repulsive *n*-alkane model with a continuous potential. The studied model is similar to that of Ryckaert and Bellemans.[1] Each methylene or methyl group is modeled as a single site placed at the position of the carbon nucleus, as shown in Fig. 1. The masses of both the methylene and methyl groups are considered equal, and set to 2.41×10^{-26} kg. The bond distance is fixed to $l = 1.53$ Å by imposing holonomic constraints.[40] The
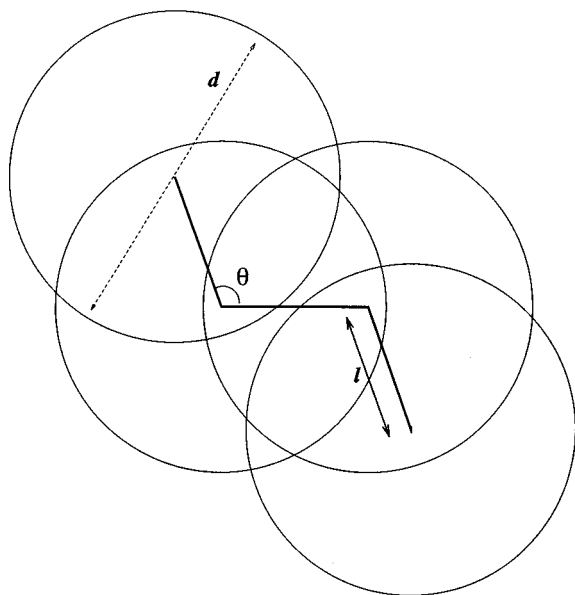
FIG. 1. Model used in this work.

value of the equilibrium bond angle C–C–C is $\theta_e = 109.5°$ and the following bending potential was used:

$$u_b(\cos\ \theta) = \tfrac{1}{2} k_\theta (\cos\ \theta - \cos\ \theta_e)^2, \qquad (35)$$

where θ is the current value of the C–C–C angle and k_θ is the force constant which has been set to 520 kJ/mol. In all the cases, the torsional potential used in the simulations is that proposed by Ryckaert and Bellemans,[1] which will be denoted as u_{RB}. Intermolecular and intramolecular interactions are given by a WCA-type potential:[33]

$$u^{WCA} = 4\epsilon\left(\left(\frac{\sigma}{r}\right)^{12} - \left(\frac{\sigma}{r}\right)^6\right) + \epsilon, \quad r < 2^{1/6}\sigma, \qquad (36)$$

$$u^{WCA} = 0, \quad r > 2^{1/6}\sigma, \qquad (37)$$

with $\epsilon/k = 72$ K and $\sigma = 3.923$ Å. Intramolecular interactions, as given by Eqs. (36) and (37), are only included between carbons separated by more than three C–C bonds. In all the studied systems the value of the temperature was T=366.88 K. During the simulation, the temperature was kept constant with the help of the Nosé–Hoover thermostat,[41] and the equations of motion were solved with the leap-frog algorithm.[42] In all the cases, the simulation sample was composed of 64 chains. The molecules were contained in a cubic box with periodic boundary conditions. The time step was set to 1.0 fs. The typical time for equilibration was 70 ps and after that the simulation run length was 700 ps. Submeans were collected every 70 ps. The results we present for the simulations are the average of the submeans. The uncertainty was estimated as the standard deviation. In addition to the MD simulations of pure WCA n-alkane models a few simulations were performed for equimolar WCA n-alkane mixtures. Simulation details are similar to that described for the pure compound simulations.

In order to compare the MD for the WCA potential with the theoretical results it is necessary to define the hard model which corresponds to the simulation model. We need:

(a) To define the hard body which corresponds to each WCA conformer.

(b) That the population of conformers at zero density of the hard model, and of the WCA model be the same. According to that, excluded volume interactions (interactions between carbons separated by more than three bonds) must be described with the same potential in both theory and simulation. Therefore, we shall use the WCA potential for describing excluded volume interactions within the theory.

For defining the hard body which corresponds to each WCA conformer (step a) each site will be replaced by a hard sphere of diameter d. We shall use the Barker–Henderson prescription[43] for obtaining the effective hard sphere diameter d, which corresponds to the WCA sites. Therefore, d is obtained at each temperature from the relation

$$d = \int_0^{2^{1/6}\sigma} (1 - \exp(-\beta u_{WCA})) dr. \qquad (38)$$

Its value for the WCA potential of this work, when evaluated at $T = 366.88$ K, is $d = 3.7109$ Å.

The population of conformers of the hard model at zero density is obtained within the RIS approximation. According to our previous treatment, the energy of the gauche conformer relative to the trans conformer, D, is temperature dependent. It can be obtained for a given torsional potential from Eq. (14) of Ref. 22. When evaluated at $T = 366.88$ K for the torsional potential of Ryckaert and Bellemans[1] it yields 3337.83 J/mol.

The theoretical EOS for the WCA model used in the MD simulations is obtained as follows:

(1) The EOS of the chain is given by Eqs. (20).

(2) The average value of the nonsphericity and volume, $\bar{\alpha}$ and $\bar{V}$, are obtained from a Monte Carlo run of an isolated chain with fixed bond lengths and angles, and with torsional degrees of freedom treated within the RIS approximation. The energy of the gauche conformer relative to the trans is 3337.83 J/mol. Excluded volume interactions are described by the WCA potential. In the MC a reptation algorithm is used for generating the conformers of the isolated chain.

(3) The nonsphericity α_i of a given conformer which appears in the Monte Carlo run is estimated from Eq. (34). The hard conformer is obtained by keeping the C–C distances to 1.53 Å and by using a hard sphere diameter of $d = 3.7109$ Å.

The reader may wonder why the WCA potential is considered for describing excluded volume effects in the MC run, instead of using a hard body potential. The explanation is as follows. When the WCA potential is used, the gg sequence is somewhat unfavorable (positive energy), whereas for the hard model this sequence is suppressed, since there is a small overlap between the first and the last carbon of the sequence. The characteristic properties (end–end distance, mean radius of gyration) of an n-alkane model in which gg sequences are permitted are different from those of another

model in which they are suppressed. Properties of chain molecules are sensitive to the details of intramolecular interactions.[34] Conformational space should be sampled in the same way in both theory and MD. Therefore, excluded volume interactions will be described by the WCA potential within the theory.

The number of steps of the MC ranges from 10^5 for short chains up to 10^6 for a chain of 600 monomers. Long runs are needed for the polymer model of 600 monomer units, since polymers of this size present long relaxation times.[44] The first half of the MC run corresponds to the equilibration of the chain, and the second half was used for obtaining averages. All calculations described in this work were performed in a workstation Alpha 3000/600 and computer times will refer to this machine. Determination of the theoretical EOS for the C_{30} chain requires about 10 min of CPU time. That should be compared with the 200 h that would require ten MD simulation runs at ten different densities. For the C_{600}, determination of the theoretical EOS took about 24 h.

The methodology described in Secs. II–IV allows one to obtain the EOS of a hard or soft repulsive polymer model.

V. RESULTS

In Table II, the compressibility factor for the repulsive models of *n*-alkanes described in Sec. IV, are presented as obtained from MD simulations and from the theory of this work. As it can be seen in Table II, the agreement between theory and simulation is remarkably good, and it does not deteriorate (at least for the *n*-alkanes considered) with the length of the *n*-alkane. In Table II, we also compare theoretical predictions for the EOS of a repulsive model of C_{50} and C_{100} with the MD results of Brown *et al.*[5] The agreement is also good. From the results of Table II it can be seen that the theory yields quantitative agreement with simulation, and in most of the cases the theoretical predictions are within the simulation uncertainty. To our knowledge, this is the first time that a theory yields quantitative agreement with simulation for the EOS of a realistic model of an *n*-alkane chain at liquidlike densities. The explanation of such a good agreement is difficult. We believe that approximations made in Sec. II concerning the estimate of $\bar{\alpha}$, and thus of the second virial coefficient of the chain, can be considered as satisfactory. However, we do not have any *a priori* reason to explain why Eq. (1) with m replaced by $2\bar{\alpha}-1$ is performing so well for *n*-alkane models. One possible explanation is that Eq. (20) predicts that virial coefficients of a flexible molecule are linear functions of the nonsphericity, and that seems to be true for short *n*-alkane models.[22] In spite of the quality of the results presented in Table II, we expect somewhat worse results for longer chains. The reason for that is that we are using the shape of the molecule as determined at zero density for describing the shape of the molecule at any density. Obviously, the shape of the molecule depends to some extent on the density. In Table III, the mean radius of gyration as obtained from the MD simulations, and from the theory are compared for several repulsive *n*-alkanes. The simulation re-

TABLE III. Mean-square radius of gyration $\langle s^2 \rangle$ of WCA *n*-alkane models (in σ^2 units) as predicted by the theory and as obtained from MD simulations of this work. Simulation results for C_{50}, and C_{100} are from Ref. 5. Reduced densities as in Table II.

n	ρ^*	$\langle s^2_{\text{MD}} \rangle$	$\langle s^2_{\text{Theory}} \rangle$
12	0.030796	0.917(4)	0.9280
12	0.076991	0.913(4)	0.9280
12	0.123185	0.909(4)	0.9280
16	0.023445	1.488(7)	1.5088
16	0.058613	1.479(7)	1.5088
16	0.093781	1.474(7)	1.5088
30	0.012773	4.06(5)	4.2042
30	0.031933	3.97(3)	4.2042
30	0.051093	3.92(10)	4.2042
50	0.04699	7.91(5)	8.44
100	0.02353	18.89(11)	23.71

sults show that the mean square radius of gyration decreases with the density, and this effect is found to be more important as the length of the chain increases. This is consistent with Flory hypothesis which state that excluded volume interactions are screened out in the dense liquid. The theory of this work predicts a radius of gyration which does not depend on density. Whereas this is reasonable for chains up to C_{100}, it is clear from the results of Table III that for longer chains that will be a poor approximation. To overcome this situation, the effect of density on the shape of the chain should be taken into account. Some attempts to overcome this problem have been performed for short[22,23] and long chains.[45]

In Fig. 2, the compressibility factor of *n*-hexane, *n*-dodecane, *n*-hexadecane, and *n*-triacontane are represented
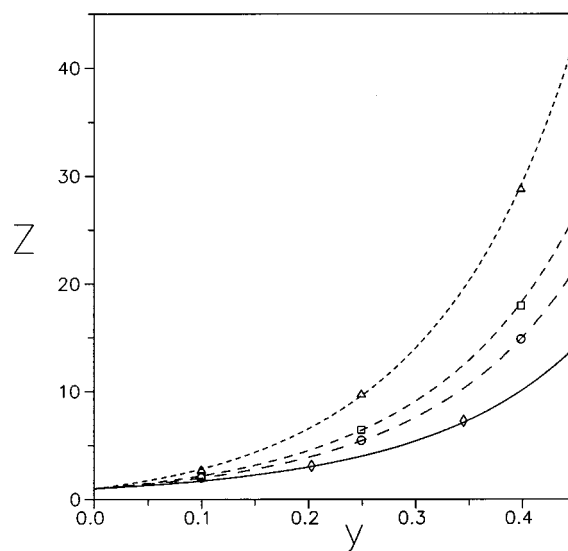
FIG. 2. Compressibility factor Z against packing fraction y for the WCA version of the *n*-alkane model of Ryckaert and Bellemans for the isotherm $T=366.88$ K. Results obtained from MD simulation (symbols) and from theory (lines) for various *n*-alkanes are presented. C_6: diamonds (MD results from Ref. 23) and full line; C_{12}: circles and long-dashed line; C_{16}: squares and dashed line, C_{30}: triangles and short-dashed line.

TABLE IV. Mean radius of curvature, surface, volume, nonsphericity parameter, effective tangent sphere number [see Eq. (6)] , *m*, average of the square of the end–end vector $\langle r^2 \rangle$, and square radius of gyration $\langle s^2 \rangle$ for *n*-alkane models. Results are given in *d* units where *d* is the BH effective hard diameter of the monomer.

n	$\bar{R}$	$\bar{S}$	$\bar{V}$	$\bar{\alpha}$	*m*	$\langle r^2 \rangle$	$\langle s^2 \rangle$
4	0.7668	6.8379	1.4275	1.1992	1.398	0.8435	0.1413
5	0.8431	8.0451	1.7276	1.2820	1.564	1.5306	0.2176
6	0.9232	9.2410	2.0272	1.3852	1.770	2.2624	0.3039
7	1.0000	10.4479	2.3263	1.4732	1.946	3.2012	0.4028
8	1.0765	11.6424	2.6252	1.5738	2.148	4.0757	0.5063
10	1.2303	14.0554	3.2235	1.7714	2.543	6.4049	0.7569
12	1.3827	16.4534	3.8220	1.9710	2.942	8.8797	1.0371
16	1.6824	21.2545	5.0191	2.3661	3.732	14.5015	1.6862
30	2.6751	38.0738	9.2083	3.6838	6.368	39.0526	4.6985
50	3.9941	62.1396	15.1967	5.4442	9.888	81.0721	10.5670
70	5.0796	86.1068	21.1792	6.8859	12.772	122.5029	16.8505
84	5.7733	102.9374	25.3687	7.8120	14.624	160.6647	21.8285
100	6.4173	122.1301	30.1516	8.6667	16.333	175.9288	25.7747
200	10.0135	242.4879	60.0930	13.4718	25.943	439.3549	62.0719
400	16.6352	482.7336	120.0184	21.7120	42.424	1426.2912	187.6450
600	18.5510	723.4109	179.9526	24.8664	48.735	1451.3465	201.2699

as a function of the packing fraction *y* defined by Eq. (22). It is seen that for a given packing fraction the pressure increases with the length of the chain. That corresponds to the idea that the nonsphericity of the molecule increases with the length of the chain. In fact, it is well known from the EOS of hard bodies arising from scaled particle theory that for a given packing fraction, the pressure increases as the nonsphericity parameter increases.[29]

The nonsphericity parameter $\bar{\alpha}$ for the model described in Sec. III, has been estimated for *n*-alkane chains up to 600 carbon atoms by using Eq. (34) and the Monte Carlo procedure described in the previous section. Results for $\bar{\alpha}$ are presented in Table IV, and in Fig. 3. For short chains (small *n*), the nonsphericity parameter increases linearly with the length of the chain, *n*. That was also found by Pavlicek and Boublik for short chains.[46] However, for large *n* the increase of $\bar{\alpha}$ with *n* is not linear. In Fig. 3, the value of $\bar{\alpha}$ for the freely jointed hard sphere model, as obtained from the second virial coefficient data of Yethiraj *et al.*,[47] is also represented. Trends in the variation of $\bar{\alpha}$ with *n* are similar for the *n*-alkane models, and for the freely jointed hard sphere model. For a given *n*, the value of $\bar{\alpha}$ is larger for the freely jointed hard sphere model than for the *n*-alkane model. This is expected, since the freely jointed hard sphere model has a larger bond length than the *n*-alkane model. The results presented in Fig. 3 show that $\bar{\alpha}$ increases with *n*. That appears to be in conflict with the idea that for large *n* the molecule can be described as a random coil of spherical shape. This idea is wrong. The shape of an *n*-alkane molecule is rather elongated (see, for instance, Fig. 1 of Ref. 35 and Fig. 7 of Ref. 48). We checked that idea in two different ways. First, a number of conformers generated during the Monte Carlo run were plotted and we found that *n*-alkane molecules are quite elongated. Second, the three principal moments of inertia of the conformers I_1^c, I_2^c, and I_3^c were analyzed. We ordered the three principal moments of inertia of the conformer so that

$I_1^c < I_2^c < I_3^c$. We found that the MC averages of I_1^c, I_2^c, and I_3^c were quite different, indicating that the individual conformers are rather anisotropic. This anisotropy is not a special feature of *n*-alkanes. It should be reminded that simulation and theoretical studies have shown that a random walk presents a rather elongated and nonspherical shape.[49] An idea of the strong anisotropy of *n*-alkane chains can be obtained by comparing the value of $\bar{\alpha}$ with the value of the nonsphericity of the all trans conformer $\alpha_{tt..t}$ (which is almost an extended linear model). For instance, for the C$_{30}$ and C$_{100}$
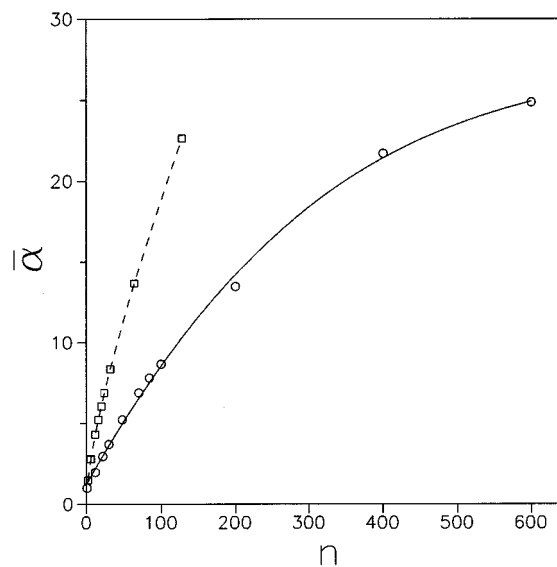
FIG. 3. Nonsphericity parameter $\bar{\alpha}$ against carbon atom number n. Open circles: $\bar{\alpha}$ for our model alkane as obtained by the MC procedure proposed in this work at *T*=366.88 K. Open squares: $\bar{\alpha}$ for the freely jointed hard sphere model as obtained from the second virial coefficients of Ref. 47. Lines through the points are only a guide to the eye.
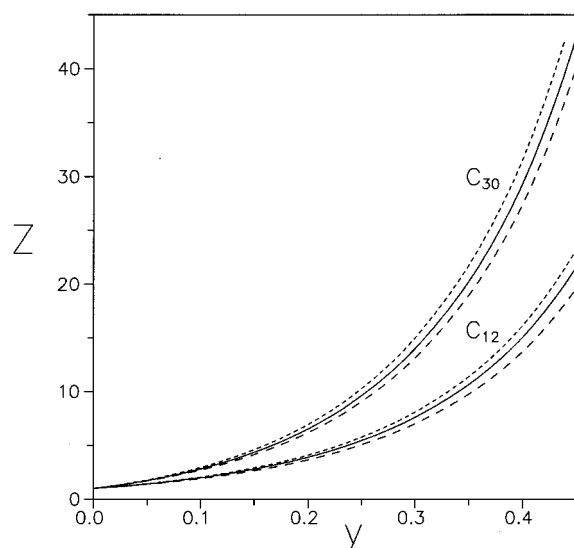
FIG. 4. Effect of bond length on the compressibility factor for C_{12} and C_{30}, as predicted by the theory presented in this work. Full line: results for our model, with $l = 1.530$ Å. Long-dashed line: results for $l = 1.299$ Å. Short-dashed line: results for $l = 1.670$ Å.

FIG. 5. Effect of bond angle on the compressibility factor for C_{12} and C_{30} as predicted by the theory presented in this work. Full line: results for our model, $\theta = 109.5°$. Long-dashed line: results for $\theta = 100°$. Short-dashed line: results for $\theta = 120°$.

n-alkanes the all trans conformers present nonsphericity values of 4.1092 and 12.1052, respectively. This should be compared with the values of $\bar{\alpha}$ presented in Table IV. It is seen that the anisotropy of the *n*-alkane is smaller than that of the all trans conformer, but of the same order of magnitude, giving an idea of the strong anisotropy of the chains. From the results of Fig. 3 it is difficult to extrapolate the behavior of $\bar{\alpha}$ at very large n.

The quality of the theoretical results presented in Table II gives us some confidence in the proposed methodology. Some questions concerning the effect of changes on the bond length, bond angle, or torsional potential on the EOS of the repulsive *n*-alkane model can be analyzed. We shall start by analyzing the effect of a change in the bond length of the molecule, when all the other parameters are kept constant. This is made in Fig. 4, where the EOS for an *n*-alkane model with $l = 1.299$ Å, $l = 1.53$ Å, and $l = 1.670$ Å are plotted. The rest of the characteristics of the model, i.e., bond angle, torsional potential, temperature, and the WCA potential (for describing excluded volume effects), correspond to those described in Sec. IV and are the same for the three bond lengths. In Fig. 5, the EOS for several *n*-alkanes models, which only differs in the internal angle between bonds, is presented. Finally, in Fig. 6, the effect of changing the torsional potential in the EOS is shown. Two torsional potentials, that of Ryckaert and Bellemans and that of Scott and Scheraga[50] (SS), are compared. For the SS torsional potential the value of the gauche energy is $D = 2207$ J/mol. The results presented in Figs. 4–6 can be summarized as follows:

(i) A decrease in the bond length provokes a decrease in the pressure for a given packing fraction.

(ii) The increase of the bond angle provokes an increase in the pressure for a given packing fraction.
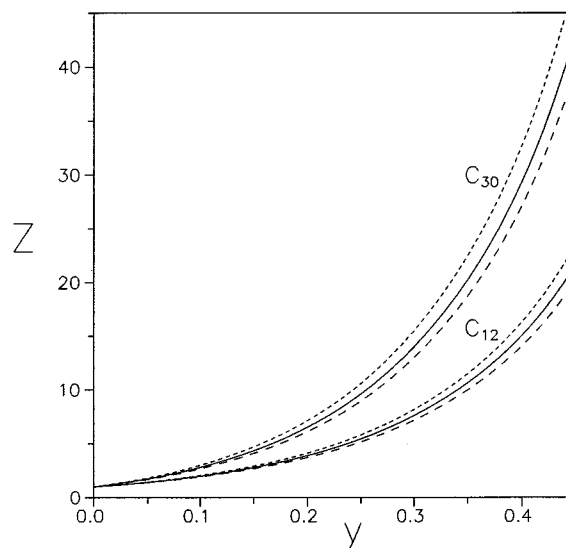
(iii) When the torsional potential makes the gauche conformer more unfavorable, then the pressure at a given packing fraction increases. In any case, the effect of changes in the torsional potential on the EOS is small.

It is important to emphasize that comparisons presented in Figs. 4–6 were performed at a constant packing fraction. For instance, when the bond length decreases in the *n*-alkane model (Fig. 4), the molecular volume and the nonsphericity parameter are reduced. Therefore, if the number density is
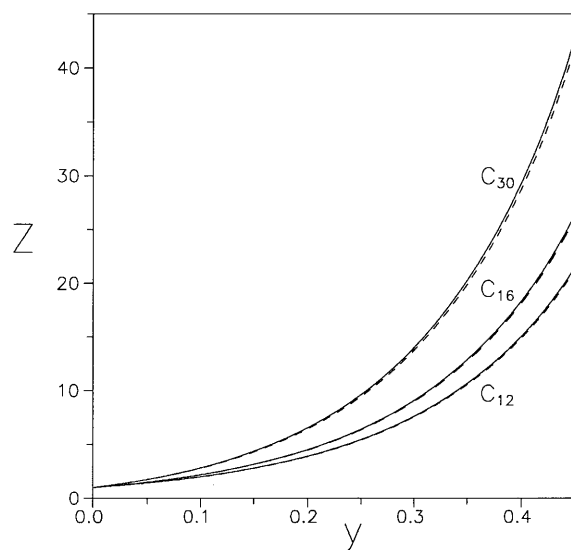
FIG. 6. Effect of the torsional potential on the compressibility factor for C_{12}, C_{16}, and C_{30}. The full line represents results using the Ryckaert–Bellemans torsional potential, while the dashed line represents results using the Scott–Scheraga potential.

TABLE V. Nonsphericity parameter α_{mixture}, and volume V_{mixture} as defined from Eqs. (39) and (40) for equimolar binary mixtures of *n*-alkane models. The equimolar mixture $8+8$ denotes the pure compound C_8.

Mixture	V_{mixture}	α_{mixture}
8+8	2.6252	1.5738
10+6	2.6254	1.5783
12+4	2.6248	1.5851
50+50	15.1967	5.4442
70+30	15.1938	5.2848
84+16	15.1939	5.0890

kept constant for two models differing only in the bond length, a strong decrease in the pressure will be observed with the shrinking of the bond length. This decrease in pressure is due to two factors, the decrease of the molecular volume and the decrease of $\bar{\alpha}$. By comparing the two models at the same packing fraction, the trivial effect on the pressure due to the change of molecular volume is removed. The results presented in Figs. 4–6, thus, represent the change in the EOS of the *n*-alkane model due to the change of shape of the molecule. A higher value of the pressure at a given packing fraction corresponds to a larger value of the nonsphericity parameter. As shown in Fig. 5, the nonsphericity parameter increases with the bond angle. The increase of the nonsphericity parameter with bond angle has also been observed in tangent hard sphere triatomic models (see Fig. 8 of Ref. 51).

Finally, we shall extend Eq. (20) to polymer mixtures. For simplicity we shall consider a binary mixture, although the treatment can be easily extended to multicomponent mixtures. The two polymers will be denoted as λ and ω, respectively. According to that, $\bar{\alpha}_\lambda$ and $\bar{V}_\lambda$ will represent the mean nonsphericity and volume of polymer λ, and a similar notation will be used for polymer ω. Let us assume that the values of $\bar{\alpha}_\lambda$ and $\bar{V}_\lambda$ are known from an MC run of an isolated chain of polymer λ, and that the same is true for the corresponding values of the chain ω. We shall define the nonsphericity and volume of the mixture, α_{mixture} and V_{mixture}, respectively, as

$$\alpha_{\text{mixture}} = x_\lambda \bar{\alpha}_\lambda + x_\omega \bar{\alpha}_\omega, \tag{39}$$

$$V_{\text{mixture}} = x_\lambda \bar{V}_\lambda + x_\omega \bar{V}_\omega, \tag{40}$$

where x_λ is the molar fraction of polymer λ and x_ω is the molar fraction of polymer ω. The theoretical EOS of the mixture will be given by Eq. (20), with $\bar{\alpha}$ and $\bar{V}$ replaced by α_{mixture}, and V_{mixture} obtained from Eqs. (39)–(40). In Table V, values of α_{mixture} and V_{mixture} for several binary mixtures are shown. In Fig. 7, the EOSs for equimolecular binary mixtures of $C_{10}+C_6$, C_8+C_8, and $C_{12}+C_4$ are represented as a function of the packing fraction. As it can be seen, the EOSs for these three binary mixtures are almost identical. This is in agreement with previous findings concerning the insensitivity of the EOS to polydispersity.[52] A comparison between simulation results and theoretical predictions for these binary mixtures is shown in Fig. 7 and in Table II. As can be seen the agreement between theory and simulation is quite good. Results for the binary mixtures $C_{50}+C_{50}$,
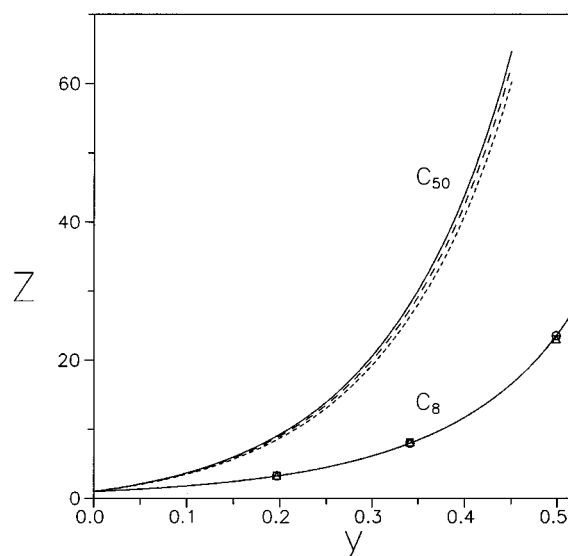
FIG. 7. Compressibility factor for equimolar mixtures of the repulsive *n*-alkane model, as predicted by the theory in this work. "C_8-sort" mixture: full line, C_8+C_8; long-dashed line, C_6+C_{10}; short-dashed line, C_4+C_{12}. With the scale of the plot the three lines are almost undistinguishable. "C_{50}-sort" mixture: full line, $C_{50}+C_{50}$; long-dashed line, $C_{30}+C_{70}$; short-dashed line, $C_{16}+C_{84}$. Symbols correspond to MD results for the C_8-sort mixture: circles C_8+C_8; squares C_4+C_{12}; triangles C_6+C_{10}.

$C_{70}+C_{30}$, and $C_{84}+C_{16}$ are also shown in Fig. 7. As it can be seen, the pressure for a given packing fraction increases in the order $C_{84}+C_{16}$, $C_{70}+C_{30}$, and $C_{50}+C_{50}$. The reason for that is that α_{mixture} increases in this order, as can be seen in Table V. To our knowledge the results presented in Fig. 7 constitute the first prediction of the EOS of a binary repulsive *n*-alkane mixture, although for other hard chain mixtures previous results have been reported.[53]

Given the success of the theory for describing the EOS of WCA *n*-alkane models it would be quite useful if the theoretical results of this work were fitted to some analytical formula. We include an appendix where such an analytical EOS for the WCA version of the Ryckaert and Bellemans model of *n*-alkanes is given.

VI. CONCLUSIONS

In this work, a new method to estimate the second virial coefficient of a hard flexible molecule is proposed. The basic idea is to average the second virial coefficient of the different conformers of the flexible molecule. To estimate the second virial coefficient of each conformer we used ideas arising from convex body theory. The proposed method requires the evaluation of the surface, volume, and mean radius of curvature of each conformer. For the mean radius of curvature, we take that of a parallelepiped with the same principal moments of inertia as the considered conformer. The surface and volume of the conformer are evaluated analytically. It is shown that the method yields reliable prediction for the second virial coefficient of different conformers of short *n*-alkane models. Moreover, the determination of the second

virial coefficient for a given conformer is quite fast. In order to estimate the second virial coefficient of a flexible chain model, a Monte Carlo simulation run of an isolated chain is performed, where the mean values of the molecular volume and second virial coefficient are computed. In this way, second virial coefficients of hard flexible *n*-alkane models up to C_{600} have been computed. It is shown that the nonsphericity increases with the length of the chain, first linearly for small *n*, and then, nonlinearly for large *n*. The increase of $\bar{\alpha}$ with *n* found for *n*-alkanes is related to the increasing anisotropy of the chains for large *n*. Molecules tend to be somewhat stretched and that explains the increases of $\bar{\alpha}$ with *n*.

The EOS of hard flexible models has also been considered. We use Wertheim's EOS for chain molecules[16,17] with the number of monomeric units, *m*, replaced by $2\bar{\alpha}-1$. Comparison with MD results of repulsive *n*-alkane models, up to C_{100}, shows that Wertheim's EOS, combined with the methodology proposed in this work, yields excellent predictions of the EOS of hard *n*-alkane models, ranging from *n*-butane up to *n*-100. Further work in order to obtain an explanation of such a good agreement is needed.

The effect of a change in bond length, bond angle, and torsional potential on the EOS is analyzed. Reduction of bond length, bond angle, and gauche energy decreases the pressure for a given packing fraction. Finally, the EOS is extended to mixtures. Good agreement between the theoretical predictions for the EOS of the considered mixtures and the simulations results was obtained.

The significance of this work is that an almost quantitative EOS can be obtained for relatively realistic repulsive *n*-alkane models. The theoretical determination of the whole EOS for an *n*-alkane model requires about 1 h of CPU time in a workstation Alpha 3000/600. The determination of the EOS of an *n*-alkane model by MD simulations would require about 100 h of CPU time. It is clear that, in such conditions, the theory is still a useful tool. The code used to perform the calculations described in this work can be obtained from the authors upon request.[54] The methodology proposed in this work may be quite useful for the application of perturbation theories to flexible molecules[55] since these theories require a good equation of state for the reference repulsive system. In particular, a better understanding of the phase equilibria of *n*-alkanes can be anticipated.

ACKNOWLEDGMENTS

APPENDIX

The theory proposed in this paper can be applied to different kinds of hard polymer models. Given the importance

TABLE VI. Coefficients of Eqs. (A2) and (A3) for the equation of state of the WCA version of the *n*-alkane model of Ryckaert and Bellemans.

v_1	0.252204	a_5	0.155984
v_2	-5.43846×10^{-3}	a_6	-2.61533×10^{-2}
v_3	3.33652×10^{-4}	a_7	3.96961×10^{-3}
v_4	-1.02932×10^{-5}	a_8	-1.72388×10^{-4}
v_5	0.277304	a_9	-1.58987×10^{-3}
v_6	5.90517×10^{-3}	a_{10}	7.82123×10^{-4}
v_7	-3.65484×10^{-4}	a_{11}	-1.27818×10^{-4}
v_8	9.97788×10^{-6}	a_{12}	5.71723×10^{-6}
a_1	0.4436	a_{13}	1.25817×10^{-5}
a_2	0.152527	a_{14}	-6.93059×10^{-6}
a_3	-2.21938×10^{-2}	a_{15}	1.09112×10^{-6}
a_4	9.57927×10^{-4}	a_{16}	-4.78837×10^{-8}

of *n*-alkanes, we shall provide in this appendix an analytical equation of state for the WCA version of the *n*-alkane model proposed by Ryckaert and Bellemans.[1] This may be useful for other workers in the area of flexible models and for future work concerning *n*-alkane models. By applying the methodology described in this paper, the values of $\bar{\alpha}$ were obtained for several *n*-alkanes with the number of carbon atoms ranging from 4 up to 100 and at several temperatures between $T=180$ and 1000 K. The obtained values of $\bar{\alpha}$ were fitted, using a least squares procedure, to the following expression:

$$T_r = T/72, \tag{A1}$$

$$\begin{aligned}
\bar{\alpha} = {}&(a_1+a_2T_r+a_3T_r^2+a_4T_r^3)+(a_5+a_6T_r+a_7T_r^2\\
&+a_8T_r^3)n+(a_9+a_{10}T_r+a_{11}T_r^2+a_{12}T_r^3)n^2\\
&+(a_{13}+a_{14}T_r+a_{15}T_r^2+a_{16}T_r^3)n^3,
\end{aligned} \tag{A2}$$

where *T* is the temperature in Kelvin and *n* is the number of carbon atoms of the *n*-alkane. We proceeded in an analogous way for $\bar{V}$ which was fitted to the expression

$$\begin{aligned}
\frac{\bar{V}}{\sigma^3} = {}&\left(\frac{d}{\sigma}\right)^3((v_1+v_2T_r+v_3T_r^2+v_4T_r^3)\\
&+(v_5+v_6T_r+v_7T_r^2+v_8T_r^3)n),
\end{aligned} \tag{A3}$$

$$T^* = \frac{T}{\epsilon/k}, \tag{A4}$$

$$\begin{aligned}
d/\sigma = {}&1.01535-3.79855\times10^{-2}\ \ln(T^*)-2.87644\\
&\times10^{-3}(\ln(T^*))^2.
\end{aligned} \tag{A5}$$

The values of the coefficients a_i and v_i are given in Table VI. Equation (A5) is a polynomial fit to the diameter obtained from the Barker–Henderson[43] prescription. If the compressibility factor of the WCA version of the Ryckaert and Bellemans *n*-alkane model for, say, $n=37$, $T=450$ K, and $\rho^*=(N/V')\sigma^3=0.02$ is needed then, T_r and T^* are obtained from Eq. (A1) and Eq. (A4), respectively, $\bar{\alpha}$ is obtained from Eq. (A2), and the packing fraction is obtained as

$$y = \rho^*\frac{\bar{V}}{\sigma^3}. \tag{A6}$$
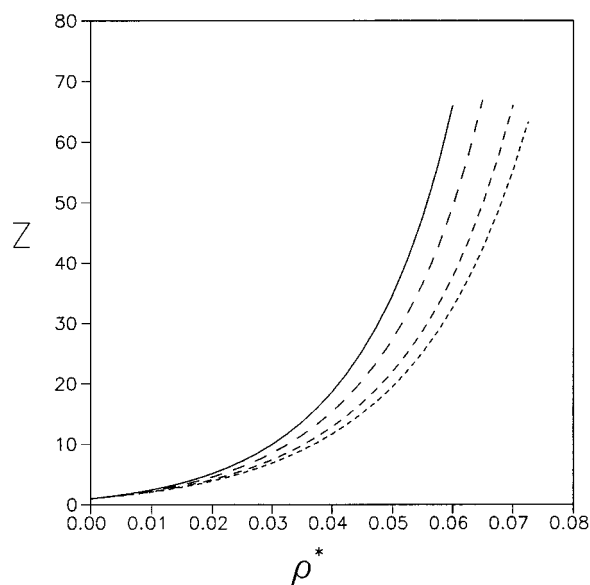
FIG. 8. Compressibility factor at different temperatures for the WCA potential of the Ryckaert–Bellemans model of C_{30}. From top to bottom results correspond to the temperatures $T = 180$, 366.88, 700, and 1000 K. The compressibility factors were obtained from Eqs. (A1)–(A6). Reduced density ρ^* as in Table II.

By substituting $\bar{\alpha}$ and y in Eq. (20), the estimate of the compressibility factor for these conditions is obtained. As an example of the application of Eqs. (A1)–(A6), in Fig. 8 the compressibility factor for the WCA of C_{30} at three different temperatures as obtained from Eqs. (A1)–(A6) is presented. Equations (A1)–(A6) should not be used for *n*-alkanes or temperatures out of the range of the fit.

[1] J. P. Ryckaert and A. Bellemans, J. Chem. Soc. Faraday Discuss. **66**, 95 (1978).

[2] N. G. Almarza, E. Enciso, J. Alonso, F. J. Bermejo, and M. Alvarez, Mol. Phys. **70**, 485 (1990).

[3] J. R. Elliott and U. S. Kanetkar, Mol. Phys. **71**, 871 (1990).

[4] D. Brown and J. H. R. Clarke, J. Chem. Phys. **92**, 3062 (1990).

[5] D. Brown, J. H. R. Clarke, M. Okuda, and T. Yamazaki, J. Chem. Phys. **100**, 1684 (1994).

[6] P. Padilla and S. Toxvaerd, J. Chem. Phys. **94**, 5650 (1991).

[7] J. Gao and J. H. Weiner, J. Chem. Phys. **91**, 3168 (1989).

[8] R. Dickman and C. K. Hall, J. Chem. Phys. **89**, 3168 (1988).

[9] B. Smit, S. Karaborni, and J. I. Siepmann, J. Chem. Phys. **102**, 2126 (1995).

[10] A. D. Mackie, A. Z. Panagiotopoulos, and S. Kumar, J. Chem. Phys. **102**, 1014 (1995).

[11] J. G. Curro and K. S. Schweizer, J. Chem. Phys. **87**, 1842 (1987).

[12] K. G. Honnell and C. K. Hall, J. Chem. Phys. **90**, 1841 (1989).

[13] C. P. Bokis, Y. Cui, and M. D. Donohue, J. Chem. Phys. **98**, 5023 (1993).

[14] E. Kierlik and M. L. Rosinberg, J. Chem. Phys. **97**, 9222 (1992).

[15] E. Kierlik and M. L. Rosinberg, J. Chem. Phys. **99**, 3950 (1993).

[16] M. S. Wertheim, J. Chem. Phys. **87**, 7323 (1987).

[17] W. G. Chapman, G. Jackson, and K. E. Gubbins, Mol. Phys. **65**, 1057 (1988).

[18] M. D. Amos, and G. Jackson, J. Chem. Phys, **96**, 4604 (1992).

[19] T. Boublik, Mol. Phys. **68**, 191 (1989).

[20] T. Boublik, C. Vega, and M. D. Pena, J. Chem. Phys. **93**, 730 (1990).

[21] J. M. Walsh and K. E. Gubbins, J. Phys. Chem. **94**, 5115 (1990).

[22] C. Vega, S. Lago, and B. Garzon, J. Chem. Phys. **100**, 2182 (1994).

[23] P. Padilla and C. Vega, Mol. Phys. **84**, 435 (1995).

[24] R. P. Sear, M. D. Amos, and G. Jackson, Mol. Phys. **80**, 777 (1993).

[25] S. Phan, E. Kierlik, and M. L. Rosinberg, J. Chem. Phys. **101**, 7997 (1994).

[26] L. A. Costa, Y. Zhou, C. K. Hall, and S. Carra, J. Chem. Phys. **102**, 6212 (1995).

[27] C. Vega, S. Lago, and B. Garzon, Mol. Phys. **82**, 1233 (1994).

[28] M. R. Wilson, Mol. Phys. **81**, 675 (1994).

[29] T. Boublik and I. Nezbeda, Collect. Czech. Chem. Commun. **51**, 2301 (1986).

[30] T. Kihara, Adv. Chem. Phys. **5**, 147 (1963).

[31] M. P. Allen, G. T. Evans, D. Frenkel, and B. M. Mulder, Adv. Chem. Phys. **86**, 1 (1993).

[32] M. Rigby, Mol. Phys. **32**, 575 (1976).

[33] J. D. Weeks, D. Chandler, and H. C. Andersen, J. Chem. Phys. **54**, 5237 (1971).

[34] J. P. Flory, *Statistical Mechanics of Chain Molecules* (Wiley, New York, 1969).

[35] L. R. Dodd and D. N. Theodorou, Mol. Phys. **72**, 1313 (1991).

[36] J. Alejandre, S. E. Martinez-Casas, and G. A. Chapela, Mol. Phys. **65**, 1185 (1988).

[37] E. Enciso, J. Alonso, N. G. Almarza, and F. J. Bermejo, J. Chem. Phys. **90**, 413 (1989).

[38] H. Hadwiger, *Altes und Neues uber konvexe Korper* (Birkhauser, Basel, 1955).

[39] L. D. Landau and E. M. Lifshitz, *Mecanica*, Vol. 1 of Curso de Fisica Teorica (Reverte, Barcelona, 1975).

[40] R. Edberg, D. J. Evans, and G. P. Morris, J. Chem. Phys. **84**, 6933 (1986).

[41] See, for example, S. Nosé, Prog. Theor. Phys. Suppl. **103**, 1 (1991).

[42] S. Toxvaerd, Mol. Phys. **72**, 159 (1991).

[43] J. A. Barker and D. Henderson, Rev. Mod. Phys. **48**, 587 (1976).

[44] K. Binder, *Observation, Prediction and Simulation of Phase Transitions in Complex Fluids*, edited by M. Baus, L. F. Rull, and J. P. Ryckaert, NATO ASI (Kluwer, Dordrecht, 1995).

[45] J. Melenkevitz, J. G. Curro, and K. S. Schweizer, J. Chem. Phys. **99**, 5571 (1993).

[46] J. Pavlicek and T. Boublik, J. Phys. Chem. **96**, 2298 (1992).

[47] A. Yethiraj, K. G. Honnell, and C. K. Hall, Macromolecules **25**, 3979 (1992).

[48] J. J. de Pablo, M. Laso, and U. W. Suter, J. Chem. Phys. **96**, 2395 (1992).

[49] K. Solc, J. Chem. Phys. **55**, 335 (1971).

[50] R. A. Scott and H. A. Scheraga, J. Chem. Phys. **44**, 3054 (1966).

[51] E. A. Muller and K. E. Gubbins, Mol. Phys. **80**, 957 (1993).

[52] S. Phan, E. Kierlik, M. L. Rosinberg, H. Yu, and G. Stell, J. Chem. Phys. **99**, 5326 (1993).

[53] J. M. Wichert and C. K. Hall, Chem. Eng. Sci. **49**, 2793 (1994).

[54] C. Vega, E-mail address: cvega at eucmos.sim.ucm.es

[55] G. Jackson and K. E. Gubbins, Pure Appl. Chem. **61**, 1021 (1989).